

## MINERALOGICAL CHARACTERIZATION OF HEMATITE FROM ALINCI, REPUBLIC OF NORTH MACEDONIA

Tena Šijakova-Ivanova, Blažo Boev

*Faculty of Natural and Technical Sciences, “Goce Delčev” University in Štip,  
Blvd. “Goce Delčev” 89, P. O. Box 201, 2000 Štip, North Macedonia  
tena.ivanova@ugd.edu.mk*

**A b s t r a c t:** In this paper preliminary mineralogical characterization of hematite from Alinci is presented. Several crystals of hematite were collected for research. The straight-forward identification of the studied mineral samples was enabled by optical microscope, SEM-EDS, ICP-MS and XRPD methods. The use of these methods showed that they are very useful methods for rapid mineral analysis contributing important analytical information. With these methods was established that the investigated mineral is hematite. Hematite crystals occur in the syenites. The size of the crystals is up to 2 cm. Crystals of hematite included small idiomorphic to hypidiomorphic crystals of rutile and ilmenite. Idiomorphic to hypidiomorphic crystals of ilmenite are corroded, relictized and separated as a solid breakdown solution in a homogeneous FeO–Fe<sub>2</sub>O hematite mass. Twinned idiomorphic aggregate of ilmenite partially cataclased into a homogeneous Fe-oxide mass also appear. Relict and corroded hypidiomorphic to allotriomorphic forms of rutile appear in a compact and homogeneous Fe-oxide hematite mass. EDS analyses on samples from Alinci show that hematite matrix contains from 1.59 to 5.89 % of Ti, whereas the rutile domains may contain from 1.15 to 1.50% of Fe.

**Key words:** hematite; ilmenite; rutile; Alinci; mineral association

### INTRODUCTION

The Alinci locality is situated near the village of Alinci, approximately 3 km from the Prilep–Bitola regional road. The site itself lies on the elevation known as Crn Kamen (Marić, 1949). The locality itself is within the Pelagonian metamorphic complex. It covers an area of 4 km<sup>2</sup> and is built up of alkali syenites, gneisses, muscovite schists and marbles. The first data on geological research at the locality of Alinci are given by Kossmat (1924), Protić (1959), Baric (1965), Bermanec & Zebec (1988), Bermanec (1992), Šijakova-Ivanova et al., 2018. Pegmatite occurrences are located in the series of alkaline syenites and gneisses. Syenite body has a fine-grained structure and a massive

texture. Fine grained syenites are grayish white. They are composed of quartz, albite, microcline, arfvedsonite, augite, aegirine, biotite, titanite, apatite and zircon. Coarse grain syenites are also found. Coarsely grain syenite are also compact, hard, with green white colour. Texture is massive. They are composed of feldspar, quartz, amphibole, pyroxene, titanite and apatite. Gneiss and quartz microcline veins have been found within the syenite body. The pegmatite occurrences are composed of follow minerals: microcline, arfvedsonite, albite, titanite, augite, zircon and apatite (Baric, 1964). Geological map of the Alinci locality is given on Figure 1.

### ANALYTICAL METHODS

Several samples of hematite were taken from the Alinci locality. Four of them were selected for our investigation. In our research following analytical methods were used: optical microscope, EM-

EDS, ICP-MS and XRPD. Microscopic examination were conducted with optical microscope – Leica DM 4500P, which is a high-end polarization microscope with intelligent light and contrast management.

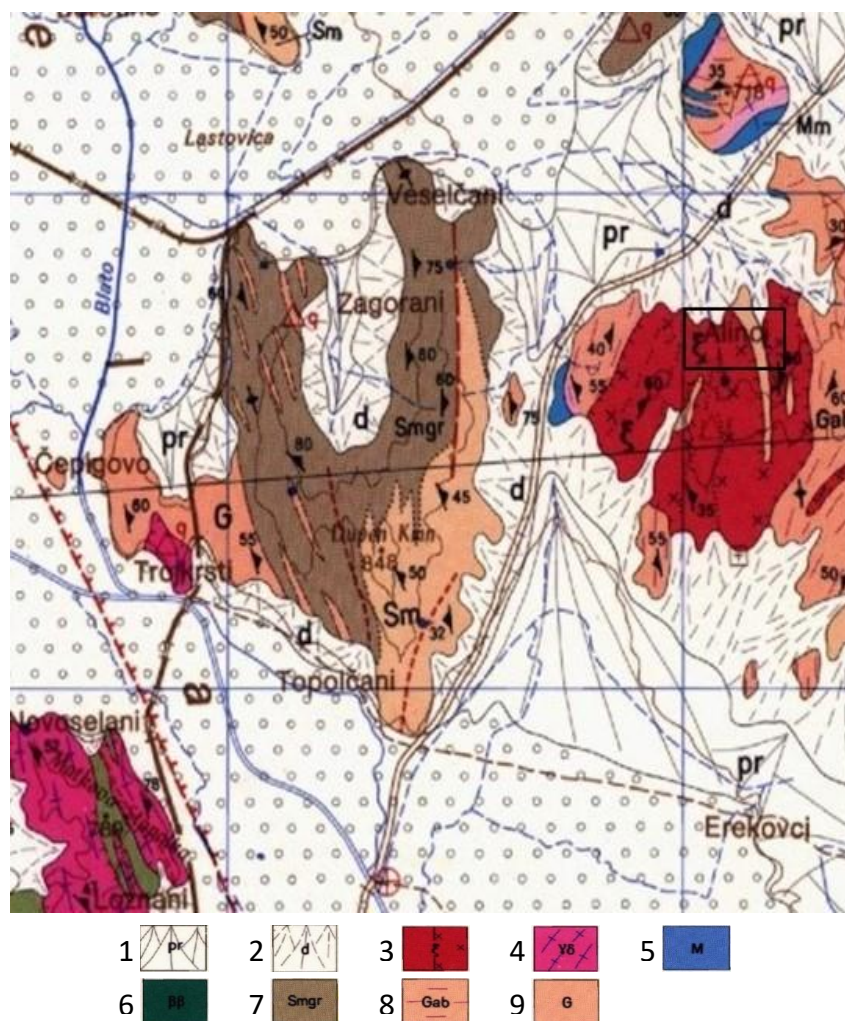


**Fig. 1.** Geological map of the Alinci locality 1:100 000 (M. Karajanović, T. Ivanovski, 1964–1972)  
 Legend: 1) proluvium; 2) diluvium; 3) syenite; 4) granodiorite; 5) marble; 6) metamorphosed diabases;  
 7) graphite schist; 8) albite gneiss; 9) gneiss

After the microscopic examinations the samples were analyzed on the Scanning Electron Microscope.

SEM-EDS analyses and electron micro-photographs were conducted using a VEGA3LMU scanning electron microscopy (SEM) increasing  $2 \times 1000\ 000$ . The study utilized semi-quantitative analysis using appropriate standards. The standards used are as follows: O:  $\text{SiO}_2$ ; Na: albite; Mg:  $\text{MgO}$ ; Al:  $\text{Al}_2\text{O}_3$ ; Si:  $\text{SiO}_2$ ; P: GaP; Ca: wollastonite; Ti: Ti; Fe: Fe; Br: KBr. The samples were sputtered by a thin layer of gold to produce surface conductivity necessary for SEM observations and EDS analysis.

Chemical composition is determined with ICP-MS. This method provides a rapid and precise means of monitoring up to 50 elements simultaneously for minor and trace-levels. The ICP-MS technique is widely regarded as the most versatile analytical technique in the chemistry laboratory. When

the sample solution is introduced into the spectrometer, it becomes atomized into a mistlike cloud. This mist is carried into the argon plasma with a stream of argon gas. The plasma (ionized argon) produces temperatures close to  $7.000\ ^\circ\text{C}$ , which thermally excites the outershell electrons of the elements in the sample.

#### *Powder x-ray diffraction*

The samples were carefully ground using an agate mortar and pestle and were prepared manually by pressing the powders in cylindrical standard containers of 16 mm diameter and 2.5 mm height, in order to obtain the flattest possible surface. The diffractograms were obtained using (Shimadzu) XRD-6100 diffractometer with Cu ( $1.54060\ \text{\AA}$ ) radiation operating at 40 kV and 30 mA. The powdered sample was scanned over the  $5\text{--}80^\circ$  range

with step size of  $0.02^\circ$  and scanning speed of  $1.2^\circ/\text{min}$ . The analyzed material is finely ground, homogenized, and average bulk composition is

determined. The most intense registered maxima in the studied powder diagrams were compared with the corresponding diagrams from PDF-2 software.

## RESULTS AND DISCUSSION

Macroscopic characteristics on the hematite are given in Figure 2. Hematite has gray-black color

and metallic luster. The size of the crystals is up to 2 cm. Hematite crystals occur in the syenites.

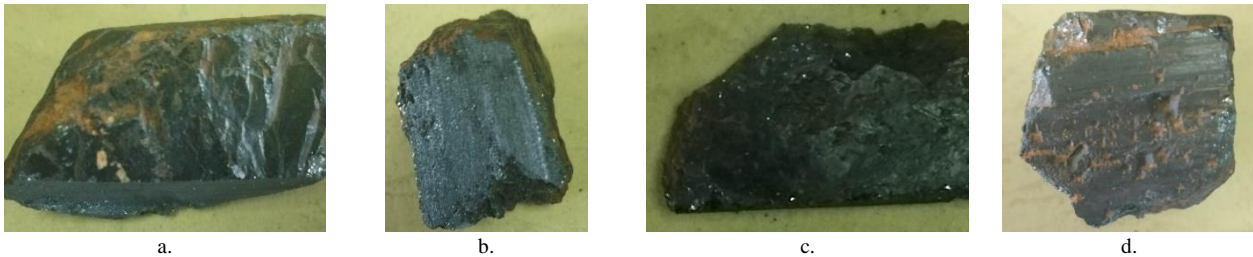
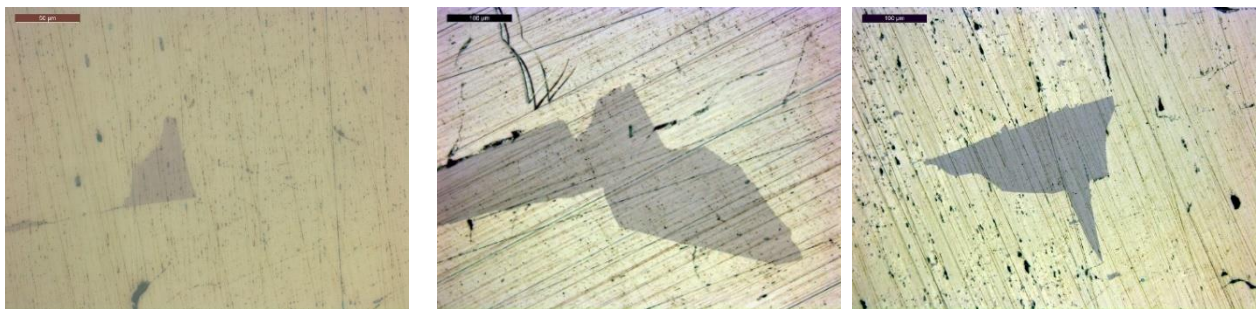


**Fig. 2.** Macroscopic characteristics of the samples: a) sample 1; b) sample 2; c) sample 3; d) sample 4

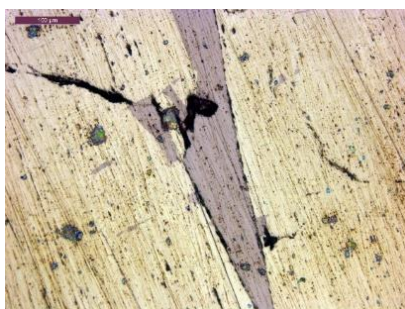
Microscopic characteristics of samples are given in Figure 3.



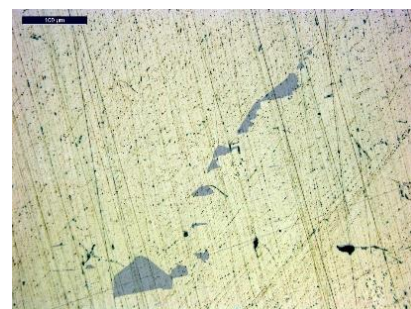
a) A single idiomorphic to hypidiomorphic crystal of ilmenite corroded and relictized and separated as a solid breakdown solution in a homogeneous  $\text{FeO-Fe}_2\text{O}_3$  hematite mass. *Mag.  $\times 400$  II*

b) Twinned idiomorphic aggregate of ilmenite partially cataclased into a homogeneous Fe-oxide mass. *Mag.  $\times 200$  II*

c) A single hypidiomorphic aggregate of rutile in a homogeneous and quite homogeneous  $\text{FeO}$  hematite matrix, *Mag.  $\times 200$  II*



d) A single hypidiomorphic aggregate of rutile in a homogeneous and quite homogeneous  $\text{FeO}$  (hematite) matrix. *Mag.  $\times 200$  II*



e) Relict and corroded hypidiomorphic to allotriomorphic forms of rutile in a compact and homogeneous Fe-oxide hematite mass. *Mag.  $\times 200$  II*

**Fig. 3.** Microscopic characteristics of the examined samples from Alinci

SEM image and EDX spectrum of hematite from Alinci are given in Figures 4 – 7.

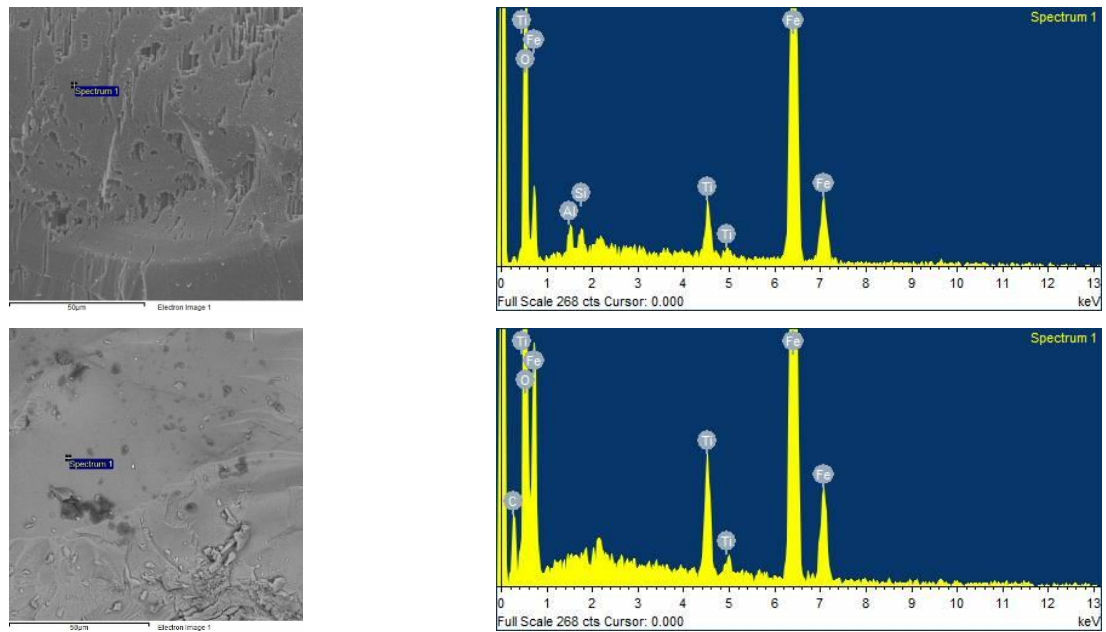


**Fig. 4.** SEM image and EDX spectrum of hematite (sample 1) from Alinci

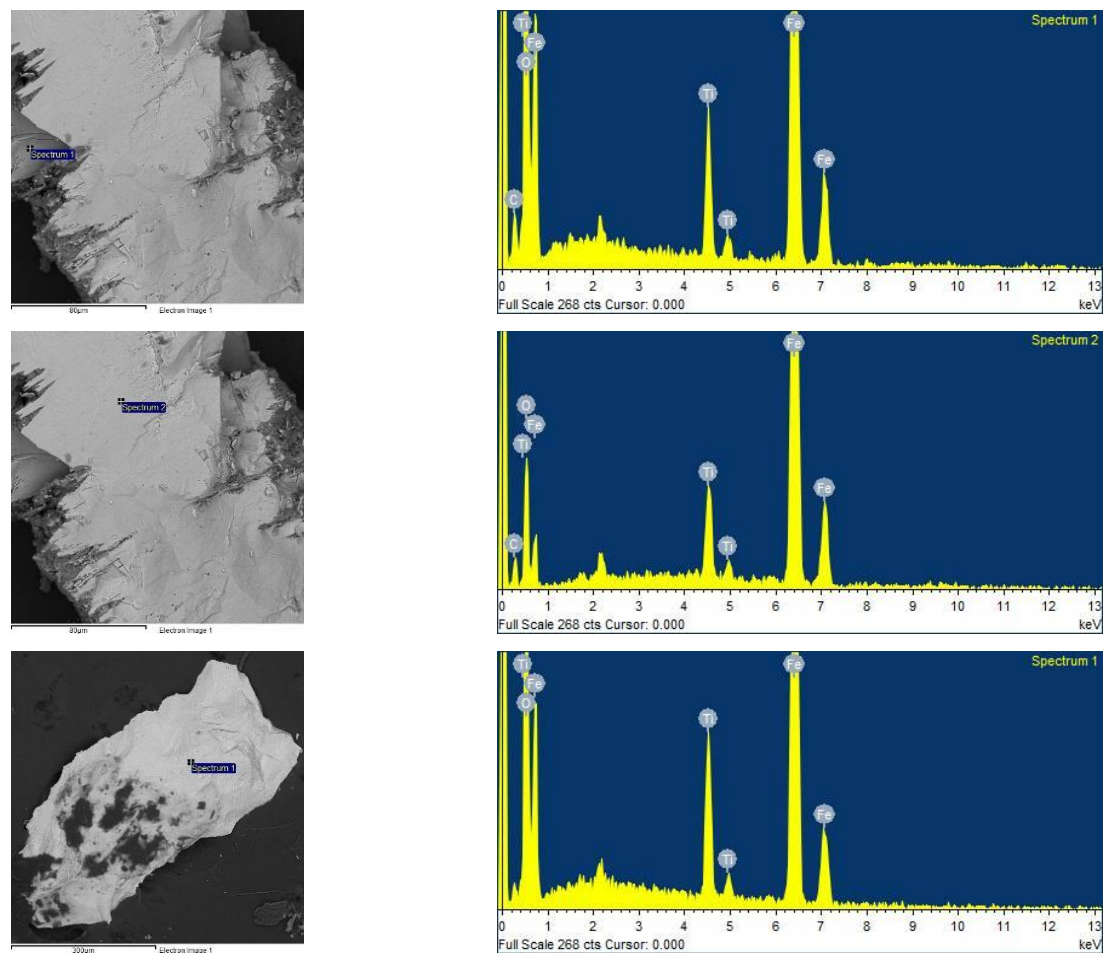


**Fig. 5.** SEM image and EDX spectrum of hematite (sample 2) from Alinci

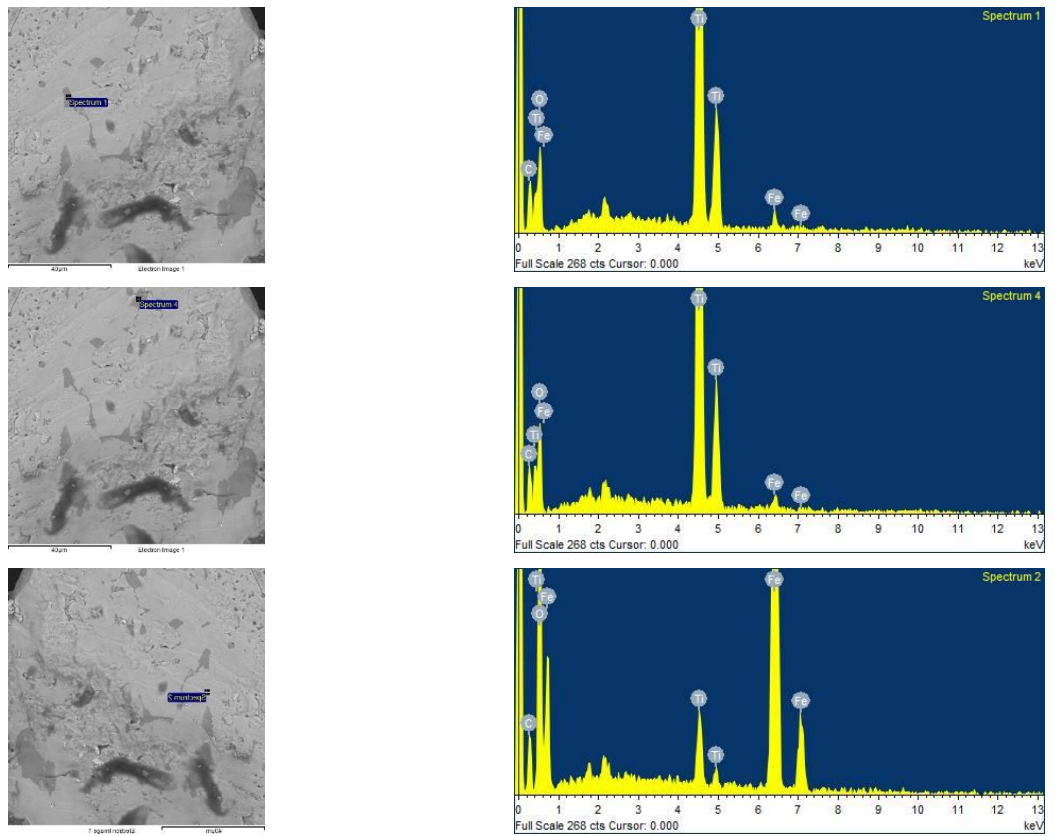


Fig. 6. SEM image and EDX spectrum of hematite (sample 3) from Alinci

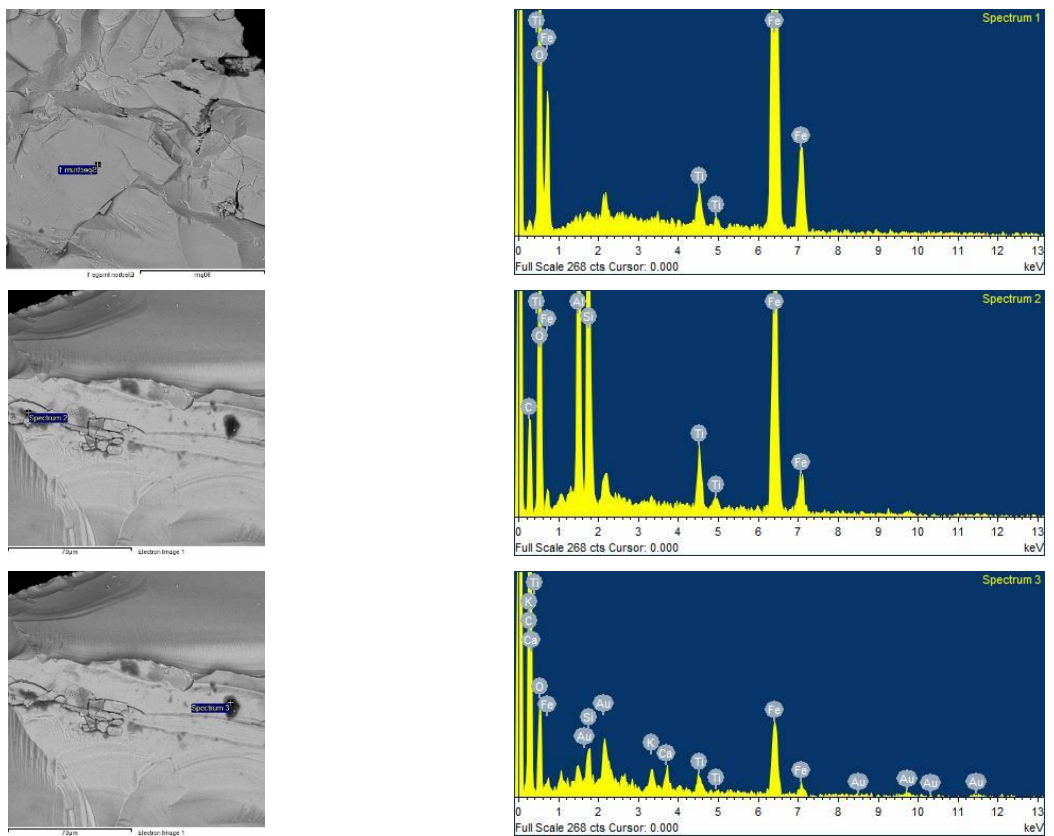


Fig. 7. SEM image and EDX spectrum of hematite (sample 4) from Alinci

Chemical composition of hematite by ICP-MS is presented in Table 1.

Table 1

*Chemical composition of hematite from Alinci*

|                                | Sample 1 | Sample 2 | Sample 3 | Sample 4 |     | Sample 1 | Sample 2 | Sample 3 | Sample 4 |
|--------------------------------|----------|----------|----------|----------|-----|----------|----------|----------|----------|
| Oxides %                       |          |          |          |          | Pd  | <1       | <1       | <1       | <1       |
| SiO <sub>2</sub>               | 2.34     | 1.93     | 2.31     | 1.84     | Ag  | <1       | <1       | <1       | <1       |
| MgO                            | 0.52     | 0.54     | 0.53     | 0.52     | Cd  | <1       | <1       | <1       | <1       |
| Al <sub>2</sub> O <sub>3</sub> | 1.88     | 1.87     | 1.80     | 1.98     | Sn  | 7.22     | 10.90    | 8.92     | 5.34     |
| CaO                            | 0.89     | 2.22     | 1.41     | 1.41     | Sb  | 11.22    | 5.86     | 4.61     | 0.40     |
| K <sub>2</sub> O               | 0.17     | 0.18     | 0.16     | 0.16     | Cs  | 0.76     | 0.85     | 0.72     | 0.73     |
| Na <sub>2</sub> O              | 0.17     | 0.22     | 0.41     | 0.11     | Ce  | 23.60    | 11.01    | 25.00    | 16.22    |
| Fe <sub>2</sub> O <sub>3</sub> | 85.14    | 85.24    | 86.31    | 86.65    | W   | 13.31    | 18.62    | 9.71     | 6.67     |
| MnO <sub>2</sub>               | 0.08     | 0.07     | 0.08     | 0.08     | Tl  | <1       | <1       | <1       | <1       |
| TiO <sub>2</sub>               | 7.47     | 7.33     | 6.55     | 6.89     | Pb  | 58.77    | 42.48    | 38.19    | 26.48    |
| Cr <sub>2</sub> O <sub>3</sub> | 0.05     | 0.05     | 0.05     | 0.06     | Bi  | <1       | <1       | <1       | <1       |
| P <sub>2</sub> O <sub>5</sub>  | 0.16     | 0.162    | 0.16     | 0.15     | Th  | <1       | <1       | <1       | <1       |
| SO <sub>3</sub>                | <0.10    | <0.10    | <0.10    | <0.10    | U   | 1.11     | 2.03     | 9.91     | 2.33     |
| LOI                            | <0.1     | <0.1     | <0.1     | <0.1     | Dy  | <1       | <1       | <1       | <1       |
| Elements mg/kg                 |          |          |          |          | Er  | 0.23     | 0.21     | 0.25     | 0.21     |
| Ni                             | 14.27    | 18.76    | 21.47    | 14.63    | Eu  | <1       | <1       | <1       | <1       |
| Co                             | 7.48     | 6.94     | 5.58     | 8.80     | Hf  | 3.20     | 3.25     | 3.39     | 3.22     |
| Cr                             | 457      | 445      | 493      | 560      | Ho  | <1       | <1       | <1       | <1       |
| Cu                             | 49.56    | 59.96    | 97.23    | 58.36    | In* | 0.33     | 0.60     | 0.50     | 0.23     |
| Zn                             | 85.16    | 70.87    | 24.61    | 42.00    | La  | 3.57     | 5.44     | 4.64     | 2.29     |
| Li                             | <1       | <1       | <1       | <1       | Lu  | <1       | <1       | <1       | <1       |
| Be                             | 1.43     | 2.19     | 1.93     | 3.91     | Nb  | 11.00    | 6.01     | 5.54     | 5.43     |
| B                              | <1       | <1       | <1       | <1       | Nd  | 2.32     | 2.93     | 2.68     | 2.84     |
| V                              | 1775     | 1959     | 2312     | 2203     | Sc* | 14.81    | 13.47    | 17.19    | 14.18    |
| Ge                             | 1.40     | 1.79     | 2.03     | 1.24     | Sm  | <1       | <1       | <1       | <1       |
| As                             | 12.09    | 12.51    | 15.58    | 13.79    | Tm  | <1       | <1       | <1       | <1       |
| Se                             | 3.43     | 3.04     | 3.34     | 3.88     | Y   | 5.59     | 5.55     | 5.68     | 5.53     |
| Rb                             | 10.58    | 8.84     | 9.13     | 7.39     | Tb  | <1       | <1       | <1       | <1       |
| Sr                             | 85.68    | 64.82    | 77.75    | 95.34    | Gd  | <1       | <1       | <1       | <1       |
| Mo                             | 3.08     | 3.94     | 2.96     | 1.32     | Pd  | <1       | <1       | <1       | <1       |

The ICP-MS results showed that the major oxide components in the sample are: Fe<sub>2</sub>O<sub>3</sub> 85.14 – 86.31%, TiO<sub>2</sub> 6.36 – 7.47%, Al<sub>2</sub>O<sub>3</sub> 1.80 – 1.98%, CaO 0.89 – 2.22%.

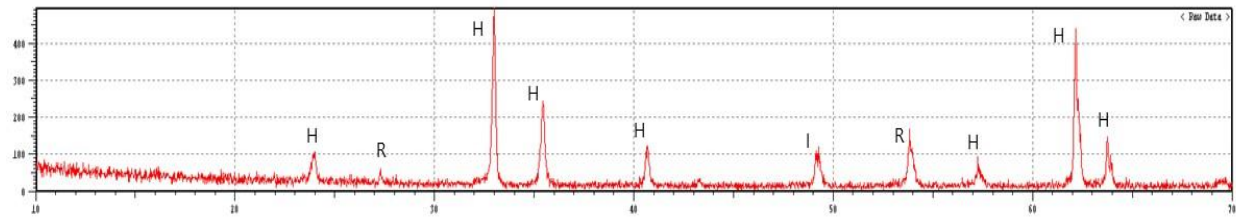
XRPD patterns of the examined hematite from Alinci are given in Figure 8.

Since hematite and ilmenite are isostructural compounds, they have spectra that are closely similar. Only a slight displacement of corresponding

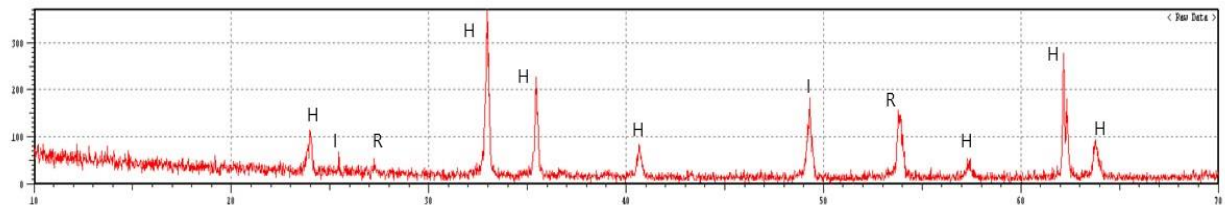
peaks is observed as a result of the small difference in the axial parameters of the two minerals. Hematite and ilmenite form at high temperature an homogeneous solid solution series with ensuing continuous variation in lattice parameters and other physical properties (Bergeron, 1980).

Both hematite (Fe<sub>2</sub>O<sub>3</sub>) and ilmenite (FeTiO<sub>3</sub>) are rhombohedral and can form a complete solid-solution series (Ilm-Hem) above ~650 °C (Lindsley, 1991).

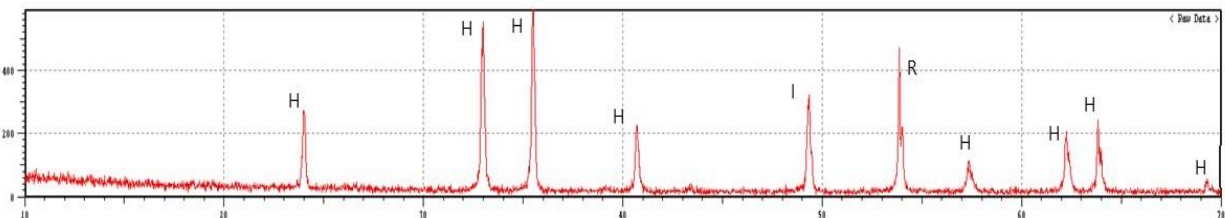
Sample 1



Sample 2



Sample 3



Sample 4

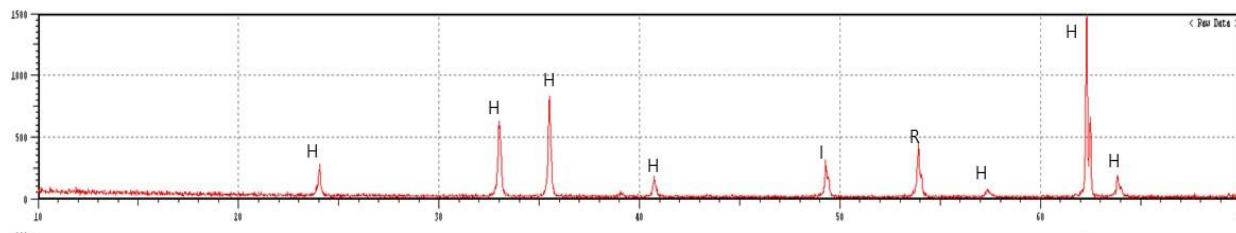


**Fig. 8.** XRPD pattern of the examined hematite from Alinci

The most common precursors for the rutile/hematite intergrowths are members of the ilmenite–hematite tie-line in  $\text{FeO-TiO}_2\text{-Fe}_2\text{O}_3$  ternary system. The phase composition in this system depends on the Fe–Ti ratio, temperature and oxygen fugacity,  $f_{\text{O}_2}$ , while the effect of pressure is less important (Buddington and Lindsley, 1964; Lindh, 1972). At the elevated temperatures, the compounds on the rhombohedral (ilm–hem) tie-line form a complete solid solution, while at lower temperatures they become immiscible, and depending on the amount of  $\text{Fe}^{3+}$ , they separate into exsolutions of hematite in ilmenite host or ilmenite in hematite host (Lindsley, 1973, 1991; Ghiorso, 1990; McEnroe et al., 2005). In nature, there are many examples of lamellar intergrowths of hematite and ilmenite from micro-

scopic grains in igneous and metamorphic rocks to large macroscopic crystals in pegmatite differentiates of mafic to ultramafic magmas (Ramdohr, 1969; Haggerty, 1971). On cooling, the activity of oxygen is increased and ilmenite may oxidize to hematite and rutile (Carmichael and Nichols, 1967; Zhao et al., 1999). Understanding the transient stages of phase transformations in this system is important in geothermometry research (Burton, 1985; Harrison et al., 2000; Meinhold, 2010).

The crystallographic study of the intergrowths has confirmed that the exsolution of rutile is entirely controlled by the hematite matrix. Consequently, one would expect that the source of Ti ions needed for the formation of intrinsic rutile lamellae must be the parent hematite. EDS analyses on different

locations show that hematite matrix contains up to 6 at % of Ti, whereas the rutile domains may contain up to 1 at % of Fe (Rečnik et al., 2015). EDS analyses on samples from Alinci show that hematite matrix contains from 1.59 to 5.89 % of Ti, whereas

the rutile domains may contain from 1.15 to 1.50% of Fe. The length of the rutile crystals ranges from 2.27 to 15.74  $\mu\text{m}$ , while the width from 1.57 to 8.51  $\mu\text{m}$ .

## CONCLUSION

After summarizing the data collected in this research, we can confirm that the studied mineral samples are hematite. The straight-forward identification of the studied mineral samples was enabled by optical microscope, SEM-EDS, ICP-MS, and XRD methods. Hematite crystals occur in the syenites. The size of the crystals is up to 2 cm. Crystals of hematite included small idiomorphic to hypidiomorphic crystals of rutile and ilmenite. Idiomorphic to hypidiomorphic crystals of ilmenite are corroded, relictized and separated as a solid breakdown solution in a homogeneous FeO–Fe<sub>2</sub>O hematite mass.

Twinned idiomorphic aggregate of ilmenite partially cataclased into a homogeneous Fe-oxide mass also appear. Relict and corroded hypidiomorphic to allotriomorphic forms of rutile appear in a compact and homogenous Fe-oxide hematite mass. The concentrations of the oxides are: Fe<sub>2</sub>O<sub>3</sub> 85.14–86.31, TiO<sub>2</sub> 6.36–7.47, Al<sub>2</sub>O<sub>3</sub> (1.80–1.98), CaO (0.89–2.22). EDS analyses on samples from Alinci show that hematite matrix contains from 1.59 to 5.89 % of Ti, whereas the rutile domains may contain from 1.15 to 1.50% of Fe.

## REFERENCES

- Barić, L. (1964): *Mineralgänge von Crni Kamen bei dem Dorf Alinci in Mazedonien*, Mineralogical Petrographic Museum of Zagreb, 23–30.
- Baric, Lj. (1965): Mineralgainge von Crni Kamen bei dem Dome Alinci in Mazedonien. – *Tscermak's Mineral.-Petrol. Mitt.* 1011-4, 368–378, Wien.
- Bergeron, M. (1980): *A Mineralogical study of the hemo-ilmenite ore from Lac Tio, Quebec*, Ministère de l'Énergie et des Ressources Gouvernement du Québec Documentation Technique.
- Bermanec, V. et al. (1992): Monazite in hydrothermal veins from Alinci, Yugoslavia, *Mineralogy and Petrology*, Volume **38**, Issue 2, pp. 139–150.
- Bermanec, V. et al. (1992): Uranium-rich metamict senaite from Alinci, Yugoslavia. *European Journal of Mineralogy* **4** (2), 331–335.
- Bermanec, V., Zebec, V. (1988): Izmjena titanita i orijentirano srastanje rutila i titanlita od Alinaca kraj Prilepa u Makedoniji, *Geol. vjesnik I*. Vol. **41**, str. 81–86, Zagreb.
- Buddington, A. F., Lindsley, D. H. (1964): Iron-titanium oxide minerals and synthetic equivalents. *J Petrol* **5**, 310–357.
- Burton, B. P. (1985): Theoretical analysis of chemical and magnetic ordering in the system Fe<sub>2</sub>O<sub>3</sub>–FeTiO<sub>3</sub>. *Am Min* **70**, 1027–1035.
- Carmichael, I. C. E., Nichols, J. (1967): Iron-titanium oxides and oxygen fugacities in volcanic rocks. *J Geophys Res* **72** (18), pp. 4665–4687, <https://doi.org/10.1029/JZ072i018p04665>
- Ghiorso, M. S. (1990): Thermodynamic properties of hematite–ilmenite–geikielite solid solutions. *Contr Mineral Petrol* **104**, pp. 645–667.
- Haggerty, S. E. (1971): Oxide textures – a mini atlas. In: Lindsley D. H. (ed.): *Oxide Minerals: Petrologic and Magnetic Significance*. *Rev Mineral* **25**, 129–219.
- Harrison, J. R., Becker, U., Redfern S. A. T. (2000): Thermodynamics of the R3<sup>-</sup> to R3<sup>c</sup> phase transition in the ilmenite–hematite solid solution. *Am Min* **85** (11–12), 1694–1705.
- Karajanović, M., Ivanovski, T. (1964–1972): Interpreter and map for the Bitola-Lerin sheet. Ed. Federal Geological Survey-Belgrade, Fund, Geological Survey-Skopje.
- Kossmat, F. (1924): *Geologie der zentralen Balkanhalbinsel*. Mit einer uebersicht des dinarischen Gebirgsbaus. Die Kriegsschauplatze 1914–1918 geologisch Dargestellt, H, 12 Berlin.
- Lindh, A. (1972): A hydrothermal investigation of the system FeO, Fe<sub>2</sub>O<sub>3</sub>, TiO<sub>2</sub>. *Lithos* **5** (4), 325–343.
- Lindsley, D. H. (1973): Delimitation of the hematite–ilmenite miscibility gap. *Geol Soc Am Bull* **84** (2), 657–662.
- Lindsley, D. H. (1991): Experimental studies of oxide minerals. In: Lindsley, D. H. (ed.): *Oxide Minerals: Petrologic and Magnetic Significance*. *Rev Mineral* **25**, 69–106.
- Marić, L. (1949): *Metamorfne kammine Bakarnega Gumna in Vesleca južno in jugozapadno od Prilepa*, Slov. akad. znan. in umetn. Ljubljana, pp. 229–246.
- McEnroe, S. A., Harrison, R. J., Jackson, M. J., Hirt, A. M., Robinson, P., Langenhorst, F., Heidelbach, F., Kasama, T., Putnis, A., Brown, L. L., Golla-Schindler, U. (2005): Lamellar magnetism: Effects of interface versus exchange interactions of nanoscale exsolutions in the ilmenite-hematite system. *J Phys: Conf Ser* **17**, pp. 154–167. DOI 10.1088/1742-6596/17/1/022.
- Meinhold, G. (2010): Rutile and its applications in Earth sciences. *Earth Sci Rev* **102**, pp. 1–28.
- Protić, M., Cvetić, S. (1959): Alkali syenite and related rocks of Crni Kamen, south of Prilep, Macedonia. *Ann. Geol. Peninsula Balkan*. **26**, 205–218.



- Ramdohr, P. (1969): *The Ore Minerals and Their Intergrowths*, 3rd edn. Pergamon Press Ltd., London.
- Rečnik, A., Stanković, N., Daneu, N. (2015): Topotaxial reactions during the genesis of oriented rutile/hematite intergrowths from Mwinilunga (Zambia). *Contrib Mineral Petrol* **169**, 19.
- Šijakova-Ivanova, T., Robeva-Čukovska, L., Jovanovski, F., Kareski, S. (2018): Mineralogical characterization of riebeckite from Alinci, Republic of Macedonia. *Geologica Macedonica*, **32** (1). pp. 75–87. ISSN 1857–8586, 0352–1206 (print).
- Zhao, D., Essene, E. J., Zhang, Y. (1999): An oxygen barometer for rutile-ilmenite assemblages: oxidation state of metamorphic agents in the mantle. *Earth Planetary Sci* **166**, pp. 127–137.

## Резиме

**МИНЕРАЛОШКА КАРАКТЕРИЗАЦИЈА НА ХЕМАТИТОТ ОД АЛИНЦИ,  
РЕПУБЛИКА СЕВЕРНА МАКЕДОНИЈА****Тена Шијакова-Иванова, Блажо Боев**

*Факултет за природни и технички науки, Универзитет „Гоце Делчев“ во Штип,  
бул. Крсте Мисирков 10-А, ѓ. фах 201, 2001 Штип, Северна Македонија  
tena.ivanova@ugd.edu.mk*

**Клучни зборови:** Алинци; хематит; илменит; рутил

Во овој труд е претставена прелиминарна минералозна карактеризација на хематитот од Алинци. Идентификацијата на испитуваните минерални примероци беше овозможена со оптички микроскоп, скенирачки електронски микроскоп, SEM/EDS – скенирачка електронска микроскопија, ICP/MS – индуктивно спрегната плазма/масена спектроскопија, и XRPD – рендгенски метод на прав. Употребата на овие методи покажа дека тие се многу корисни за брза анализа на минерали придонесувајќи важни аналитички информации. Со овие методи се утврди дека испитуваниот минерал е хематит. Хематитот се појавува во кристали со големина до 2 cm. Кристалите на хематит вклучу-

ваат мали идиоморфни до хиподиоморфни кристали на рутил и илменит. Наместа кристалите на илменит се кородирани, реликтизирани и одвоени како цврст раствор на распаѓање во хомогена FeO–Fe<sub>2</sub>O хематитска маса. Се појавуваат и идиоморфни агрегати на илменит делумно катаклазиран во хомогена маса на Fe-оксид. Реликтните и кородирани хиподиоморфни до алотриоморфни кристали на рутил се појавуваат во компактна и хомогена хематитска маса на Fe-оксид. SEM-EDS-анализите на примероците од Алинци покажуваат дека матриксот на хематитот содржи од 1,59 до 5,89 % Ti, додека кристалите на рутилот содржат од 1,15 до 1,50 % Fe.

